

# Non-Additive Ion Effects Drive Both Collapse and Swelling of Thermoresponsive Polymers in Water

Ellen E. Bruce,<sup>†,§</sup> Pho T. Bui,<sup>‡,§</sup> Bradley A. Rogers,<sup>‡</sup> Paul S. Cremer,<sup>\*,‡,¶</sup> and Nico F. A. van der Vegt<sup>\*,†</sup>

<sup>†</sup>*Eduard-Zintl-Institut für Anorganische und Physikalische Chemie, Center of Smart Interfaces, Technische Universität Darmstadt, Alarich-Weiss-Straße 10, D-64287 Darmstadt, Germany*

<sup>‡</sup>*Department of Chemistry, The Pennsylvania State University, University Park, PA 16802, USA*

<sup>¶</sup>*Department of Biochemistry and Molecular Biology, The Pennsylvania State University, University Park, PA 16802, USA*

<sup>§</sup>*Contributed equally to this work*

E-mail: psc11@psu.edu; vandervegt@cpc.tu-darmstadt.de

## Abstract

When two salts containing a weakly and a strongly hydrated anion are mixed in an aqueous solution, their combined effect is non-additive. This complex response to the introduction of salts is reflected in the lower critical solution temperature (LCST) of thermoresponsive polymers. Herein, we report the LCST of poly(*N*-isopropylacrylamide) with a fixed concentration of Na<sub>2</sub>SO<sub>4</sub> and a variable concentration of NaI. Using molecular dynamics simulations and vibrational sum frequency spectroscopy, we demonstrate

that in the presence of a strongly hydrated anion ( $\text{SO}_4^{2-}$ ), the otherwise weakly hydrated anion ( $\text{I}^-$ ) begins to behave like a strongly hydrated anion at low concentrations of  $\text{I}^-$ . This behavior can be attributed to the partitioning of the cations ( $\text{Na}^+$ ) to the counterion cloud around the strongly hydrated anion, leaving the weakly hydrated anion more hydrated. However, at higher concentrations of the weakly hydrated anion, it is actually forced out of solution by the strongly hydrated anion. Thus, the LCST behavior of PNiPAM involves competing roles for ion hydration and polymer-iodide interactions. This concept can be generally applied to mixtures containing both a strongly and a weakly hydrated anion from the Hofmeister series.

## Introduction

Traditionally, ions have been classified as either strongly or weakly hydrated and ranked according to the Hofmeister series.<sup>1,2</sup> A common ordering for the anions can be seen in Figure 1. Weakly hydrated anions (right side of the series) are driven to non-polar environments such as air/water interfaces<sup>3</sup> or polymer surfaces.<sup>4-6</sup> Strongly hydrated anions (left side of the series) prefer the bulk water environment instead. However, it will be shown in this work that the affinity of a weakly hydrated anion for water can be enhanced in the presence of a second strongly hydrated anion in a concentration-dependent fashion. As such, the current Hofmeister series needs to be revised to account for weakly hydrated anions' bifurcated behavior in mixed salt solutions (Figure 1).

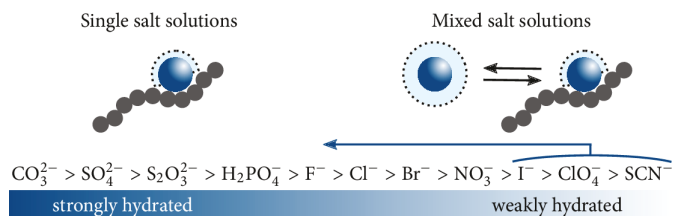


**Figure 1.** A weakly hydrated anion ( $I^-$ ) interacts with hydrophobic surfaces in single salt solutions. In mixed salt solutions, the weakly hydrated ion retains its affinity for the hydrophobic surface but also increases its water affinity due to its flexible hydration shell being able to bind excess water and act like a more strongly hydrated anion (blue arrow going to the left).

The ability to shift the balance of anion affinity for bulk water versus non-polar environments can be exploited to regulate aqueous polymer solubility. The total effect of the salt on polymer solubility is related to the behavior of both the anion and the cation. Specific interactions of anions and cations have traditionally been considered independent and additive. This idea goes back to the pioneering work of Guggenheim<sup>7,8</sup> and others<sup>9-11</sup> and is commonly used today to rationalize the actions of Hofmeister ions in chemistry and biology. Additionally, the assumption of additivity is consistent with the behavior of many single salts in the Hofmeister series.<sup>12,13</sup> Very recently, however, it has been argued that not only polymer-ion or protein-ion but also ion-counterion interactions in the bulk solution and at the polymer/protein surface can affect the polymer phase transition in a non-additive fashion.<sup>14,15</sup> For example, deviations from additivity have been observed in systems containing guanidinium cations due to the ability of these cations to form ion pairs at the macromolecule surface (cooperative binding).<sup>16,17</sup> That is, the cation can, when it is paired with different anions at opposite ends of the anionic Hofmeister series, cause either polymer swelling or collapse.

Compared to single salts, fewer studies have focused on salt mixtures. Non-additive effects on aqueous polymer solubility in mixed salt solutions have been reported for poly(propylene oxide) (thermodynamic measurements).<sup>18</sup> Additionally, non-additive effects in mixed salt solutions have been shown to drive weakly hydrated anions to the air/water interface when strongly hydrated anions are also present (spectroscopic measurements and molecular dynamics (MD) simulations).<sup>19</sup> Although interesting effects from mixed salt solutions were observed in both of these works, the mechanisms involved are complex, and the entire range of the Hofmeister series has not been explored. In other words, there are still numerous non-additive effects that have yet to be discovered.

Herein, we report ion-specific effects on the lower critical solution temperature (LCST) of poly(*N*-isopropylacrylamide) (PNiPAM) in mixed electrolyte solutions containing NaI and Na<sub>2</sub>SO<sub>4</sub>, and compare these results with mixtures of NaI with NaCl, as well as NaCl with

$\text{Na}_2\text{SO}_4$ . The most pronounced non-additive features were observed for the combination of a weakly hydrated salt ( $\text{NaI}$ ) and a strongly hydrated salt ( $\text{Na}_2\text{SO}_4$ ). Significantly, it was found that ion hydration and polymer-anion interactions can be regulated in the presence of the weakly and strongly hydrated mixed salts, leading to both collapse and swelling transitions of the polymer. The underlying mechanisms are addressed using atomic-level insights obtained from MD simulations and vibrational sum frequency spectroscopy (VSFS). Figure 2 schematically depicts the collapse and swelling mechanisms that are proposed. At low  $\text{NaI}$  concentration (region I), using  $\text{Na}_2\text{SO}_4$  as the background salt does not significantly affect the interaction between iodide and the polymer. Counterintuitively, the polymer collapses more readily. Specifically, in the presence of  $\text{Na}_2\text{SO}_4$ , the introduction of  $\text{NaI}$  causes some sodium ions to partition to the counterion cloud around sulfate. This results in a lower counterion density around iodide and leaves iodide more hydrated. As such, the effect of polymer-iodide interaction is counterbalanced by ion hydration in the bulk which provides the driving force for polymer collapse.<sup>20</sup> This effect is saturable and upon further addition of  $\text{NaI}$ , a re-entrant behavior of the polymer is observed in region II. Under these conditions, the strongly hydrated salt ( $\text{Na}_2\text{SO}_4$ ) affects the solubility of the more weakly hydrated salt ( $\text{NaI}$ ), which in turn adsorbs to a greater extent to the polymer/water interface. This is in accordance with the mechanism (one salt salts out the other) proposed in earlier work.<sup>19</sup> When the  $\text{NaI}$  concentration is increased even further (region III), the polymer again collapses, driven by the depletion of hydrated ions. These non-additive ion effects will be discussed in detail below. They shed new light on Hofmeister ion chemistry and potentially provide new insights into a broad range of complex mixed electrolyte solutions such as ocean water and dense cellular environments as well as man-made multicomponent ion solutions in a chemistry laboratory.<sup>21-23</sup>

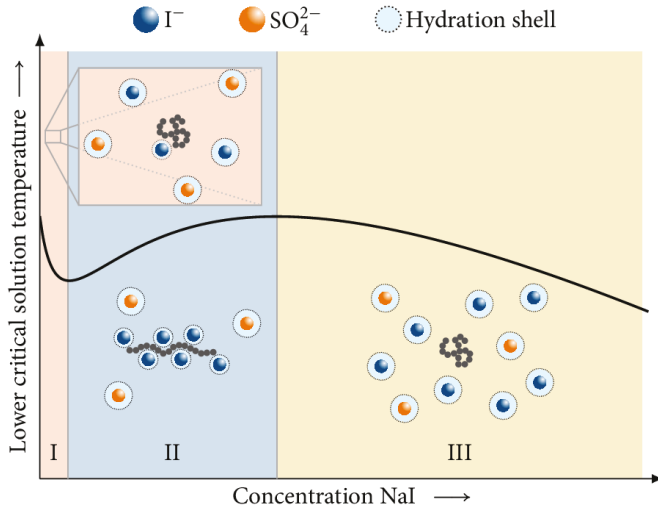


**Figure 2.** Mechanisms and driving forces for the collapse and swelling of thermoresponsive polymers in aqueous mixed electrolyte solutions containing a fixed concentration of a strongly hydrated salt ( $Na_2SO_4$ ) and an increasing concentration of a weakly hydrated salt (NaI). The iodide-water affinity changes in the presence of  $Na_2SO_4$ . This occurs due to the flexibility of iodide's hydration shell and leads to strongly non-linear behavior in the lower critical solution temperature of the polymer. In region I, enhanced iodide-water affinity drives salting out behavior. In region II,  $SO_4^{2-}$  salts out  $I^-$  which in turn becomes enriched at the polymer/water interface. In region III, excess ion hydration drives salting out again.

## Results and discussion

### The lower critical solution temperature of PNiPAM in aqueous salt solutions.

PNiPAM displays an inverse phase transition above its LCST. Herein, we systematically investigated the change in the LCST of PNiPAM in single and mixed salt solutions. The LCST was determined from measuring the turbidity change of polymer solutions as a function of temperature. More information on the LCST measurements can be found in the Supporting Information. Experimental LCST data are shown in Figure 3a. In the absence of  $Na_2SO_4$  as the background salt, the LCST of PNiPAM initially increases when NaI is added, reaches a maximum, and then decreases. This result agrees with earlier observations.<sup>4</sup> In mixed salt solutions, the solubility of PNiPAM displays more complex behavior. The specific effects depend on the concentration of NaI, the type of added salt (the background salt) as well as its concentration. At the highest  $Na_2SO_4$  background concentration that was used, the NaI concentrations can be divided into three regions. The  $0.0 - 0.1\text{ m}$  ( $0 - 100\text{ mM}$ ) range for NaI is referred to as region I,  $0.1 - 0.6\text{ m}$  ( $100 - 600\text{ mM}$ ) NaI as region II and  $> 0.6\text{ m}$

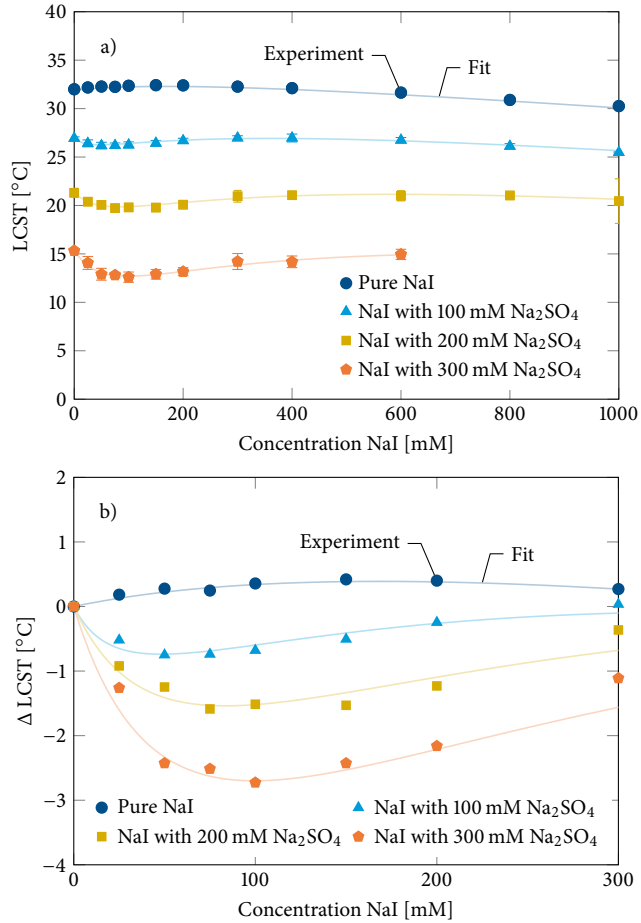


**Figure 3.** a) The lower critical solution temperature (LCST) and b) the change in LCST ( $\Delta$ LCST) of PNiPAM upon the addition of NaI with 0 mM, 100 mM, 200 mM and 300 mM Na<sub>2</sub>SO<sub>4</sub> as the background salt. Note that  $\Delta$ LCST is only shown for data points within the 0 – 300 mM NaI range in order to highlight the dip in the LCST. The error bars are calculated from sample standard deviations from three sets of measurements. See Figure S1 for the error bars corresponding to the  $\Delta$ LCST values. The fit corresponds to the empirical model given in Equation 1. The fitting parameters are reported in Table 1.

(> 600 mM) NaI as region III. For the other two lower  $\text{Na}_2\text{SO}_4$  concentrations, the boundary between region II and III shifts to lower NaI concentration. The concentrations are reported in molarity for the experimental data and in molality for simulations. The difference between the two concentration scales is negligible within the range considered in these study. In the presence of  $\text{Na}_2\text{SO}_4$  as the background salt, the LCST decreases in region I with increasing NaI concentration. This is in marked contrast to the increase observed in the pure NaI system. Upon further increase in NaI concentration, the LCST increases (region II) and then eventually decreases (region III). The magnitude of the initial decrease, which is manifest as a dip, is dependent on the background salt concentration. For comparison,  $\Delta\text{LCST}$ , defined as the change in the LCST upon the addition of NaI, is shown in Figure 3b. As can be seen, the dip becomes more pronounced as the the concentration of the background salt is increased.

The LCST of PNiPAM as a function of NaI concentration can be modeled empirically by

$$T = T_0 + ac_{\text{salt}} + \frac{B_{\text{max},1}c_{\text{salt}}}{K_{\text{D},1} + c_{\text{salt}}} + \frac{B_{\text{max},2}c_{\text{salt}}}{K_{\text{D},2} + c_{\text{salt}}}, \quad (1)$$

where  $T_0$  is the LCST in the absence of NaI, and  $ac_{\text{salt}}$  (with  $c_{\text{salt}}$  being the NaI concentration) is a linear term related to the surface tension of the hydrophobic polymer/water interface. The third term is a Langmuir binding isotherm which quantifies the increase in the LCST from the initial LCST ( $T_0$ ) due to iodide adsorption to the PNiPAM chain. The dissociation constant ( $K_{\text{D},1}$ ) quantifies the strength of the iodide adsorption process, which at saturation represents the maximum increase in the LCST ( $B_{\text{max},1}$ ). The fourth term, needed to describe the data for mixed salt solutions, is reminiscent of a Langmuir binding isotherm, but originates from ion hydration. This term quantifies the decrease in the LCST due to iodide binding more water and has a negative  $B_{\text{max},2}$  value. The LCST of PNiPAM in single electrolyte solutions can be fully explained by the first three terms and has been utilized previously.<sup>4</sup> See Table 1 for the fitting parameters and Supporting Information for

more information about the fitting.

**Table 1.** Fitting parameters ( $T_0$ ,  $a$ ,  $B_{\max,1}$ ,  $K_{D,1}$ ,  $B_{\max,2}$  and  $K_{D,2}$ ) for the empirical lower critical solution temperature model of PNiPAM in NaI and mixtures of NaI with  $\text{Na}_2\text{SO}_4$  given by Equation 1.

	Na <sub>2</sub> SO <sub>4</sub> concentration [mM]			
	0	100	200	300
$T_0$ [°C]	31.9	27.0	21.4	15.4
$a$ [°C/mM]			$-4.2 \cdot 10^{-3}$	
$B_{\max,1}$ [°C]	3.1	6.9	14.9	23.8
$K_{D,1}$ [mM]			308.1	
$B_{\max,2}$ [°C]	—	-2.5	-8.6	-15.9
$K_{D,2}$ [mM]	—	33.8	81.0	96.0

**Polymer-ion interactions.** To elucidate the observed effects on the LCST, we analyzed the number of iodide ions in proximity to a PNiPAM 5-mer (oligomer) using MD simulations. Details concerning the simulations and the force fields can be found in the Methods section and in Table S1 in the Supporting Information, respectively. The proximity is defined from the first peak in the proximal radial distribution function between the oligomer surface and iodide (not shown here). The number of iodide ions in proximity to the oligomer in region I (0.1 m NaI) is not affected by the  $\text{Na}_2\text{SO}_4$  background salt (see Figure 4). Hence, PNiPAM-iodide interactions at low NaI concentration are independent of the  $\text{Na}_2\text{SO}_4$  concentration. Despite the fact that these favorable interactions remain unaffected, the polymer actually collapses more readily.

By contrast, simulations show that in regions II and III,  $\text{Na}_2\text{SO}_4$  pushes iodide toward the PNiPAM/water interface. This agrees with the observed increase in the  $B_{\max,1}$  value as the  $\text{Na}_2\text{SO}_4$  concentration is increased (see Table 1). The favorable polymer-iodide interactions contribute to the observed increase in the LCST in the system with  $\text{Na}_2\text{SO}_4$  in region II. In a mixed electrolyte solution containing a weakly and a strongly hydrated salt, one salt may salt out the other, as has previously been demonstrated by examining ions at the air/water interface with a combination of photoelectron spectroscopy and MD simulations.<sup>19</sup> Our simulations confirm that the surface enhancement of the large polarizable anion ( $\text{I}^-$ ) is driven by the strongly hydrated ion ( $\text{SO}_4^{2-}$ ). As such, the observed increase in the LCST results from a forced iodide adsorption effect. When the NaI concentration is increased

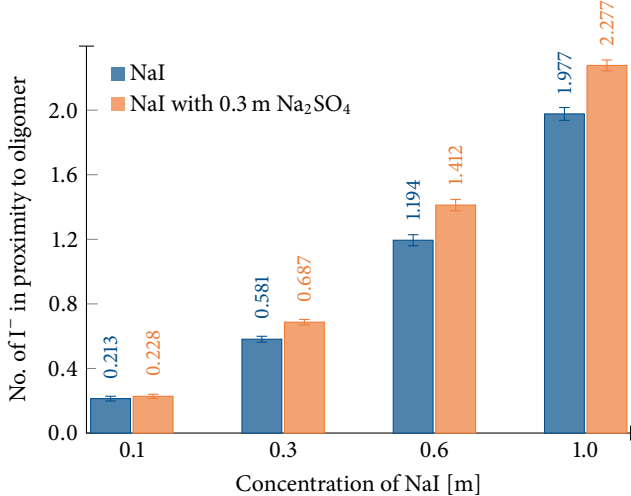


**Figure 4.** The number of iodide ions in proximity to the PNiPAM oligomer with different concentrations of NaI in the absence (blue bars) and presence (orange bars) of  $Na_2SO_4$ . The proximity is defined by the first peak in the proximal radial distribution function between the oligomer surface and iodide and is equal to 0.52 nm. The error bars are error estimates calculated from 20 blocks and sample standard deviations.

further with 100 mM and 200 mM  $Na_2SO_4$  as the background salt, the LCST reaches a maximum after which it again decreases (see Figure 3a). With 300 mM  $Na_2SO_4$  as the background salt, this decrease is not observed, but would presumably occur at a higher NaI concentration, if the solubility limit were not reached. With increasing NaI concentration, increasing iodide adsorption (see Figure 4) drives polymer swelling, while enhanced ion-water affinity at higher total salt concentration drives polymer collapse. In the presence of 100 mM and 200 mM  $Na_2SO_4$ , enhanced ion-water affinity is the dominant driving force in region III.

The findings from the MD simulations concerning favorable polymer-iodide interactions in region II and region III can be further supported by VSFS measurements. To this end, a Gibbs monolayer of PNiPAM at the air/water interface was examined. More information on the VSFS measurements can be found in the Supporting Information. Full spectra under various salt conditions in the subphase are provided in Figure S2a and Figure S2b. Information on the peak assignments and intensities can also be found in the Supporting Information (Table S2 and Table S3). Figure 5a shows the water region ( $3000 - 3800\text{ cm}^{-1}$ ) of VSFS spectra for PNiPAM at the air/water interface under three salt conditions. The spectra are dominated by two broad features at  $3200$  and  $3400\text{ cm}^{-1}$ , consistent with previous studies

of this interface.<sup>24</sup> The  $3200\text{ cm}^{-1}$  peak reports on the symmetric OH stretch mode of more ordered water molecules,<sup>25–27</sup> while, the peak around  $3400\text{ cm}^{-1}$  is indicative of the presence of water molecules with less ordered hydrogen-bonds.<sup>25–27</sup> It has been previously shown that this lower coordination water population ( $3400\text{ cm}^{-1}$ ) is closer to the interface because that is where registry between interfacial water molecules and hydrogen bond donors/acceptors from adjacent organic or inorganic layers is most easily disrupted.<sup>28</sup> Further away from the interface, it is possible to achieve more tetrahedral water structure, giving rise to peak around  $3200\text{ cm}^{-1}$ .<sup>28</sup> As such, the  $3200\text{ cm}^{-1}$  feature represents water molecules that are further away from the polymer surface and are aligned by the interfacial potential, while the  $3400\text{ cm}^{-1}$  feature arises mostly from the water structure in the inner hydration shell of the polymer, adjacent to the polymer/water interface.

Upon the introduction of NaI to the subphase, the water peaks change in a complex fashion. The oscillator strength of the  $3400\text{ cm}^{-1}$  peak monotonically increases with increasing NaI concentration due to better alignment of water molecules at the polymer surface caused by  $\text{I}^-$  adsorption (red curve in Figure 5b). Compared to the pure NaI case (see Figure S2c), the upper limit of the oscillator strength is higher in the presence of  $\text{Na}_2\text{SO}_4$ . This indicates more extensive polymer-iodide interactions and is reflected in the higher  $B_{\max,1}$  value in the presence of  $\text{Na}_2\text{SO}_4$  (see Table S4). This supports the claim that the background salt causes an increase in polymer-iodide interactions as reported in Figure 4.

**Anion-water and ion pairing affinities.** Markedly different behavior, namely a decrease followed by an increase in both the intensity and the oscillator strength of the  $3200\text{ cm}^{-1}$  peak is observed in mixed salt solutions (Figure 5a and Figure 5b). The dip in the oscillator strength (orange curve in Figure 5b) correlates to the dip in the LCST. However, it should be noted that the minimum occurs at a lower NaI concentration. Presumably, this difference originates not only from the difference in the techniques employed, but also from the difference in the binding sites being probed for the polymer in bulk (LCST measurements) and at the air/PNiPAM/water interface (VSFS measurements). In pure NaI

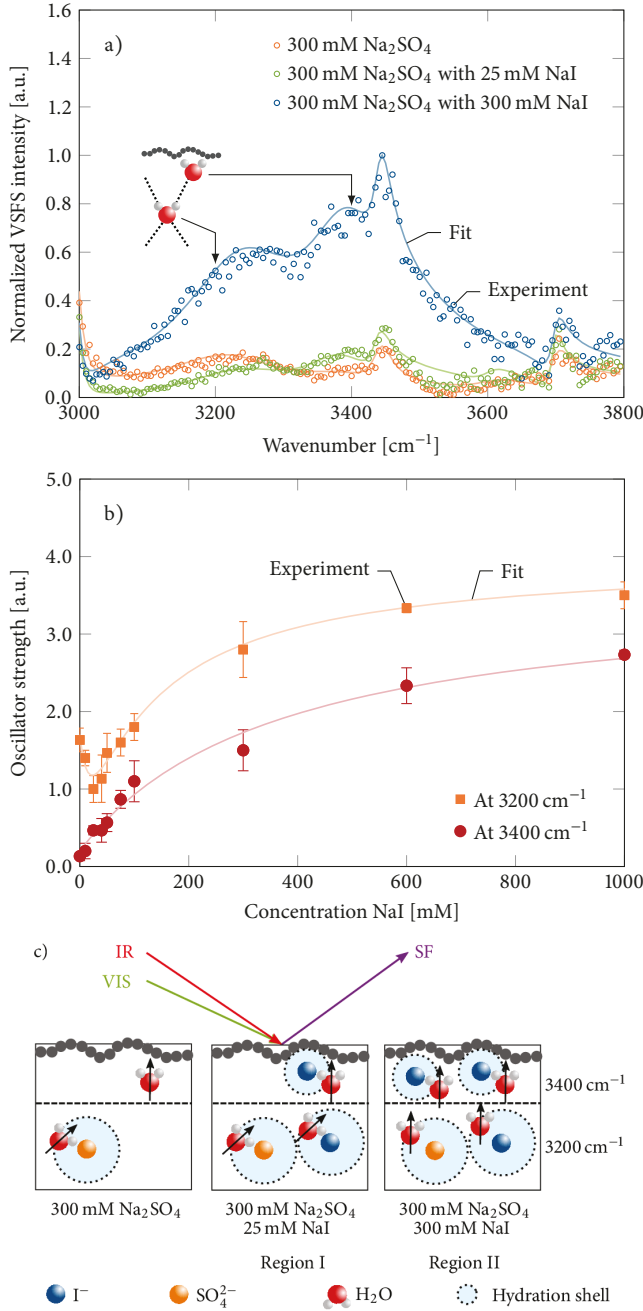


**Figure 5.** a) Vibrational sum frequency spectroscopy (VSFS) spectra of the water region (3000–3800 cm<sup>-1</sup>) of a PNiPAM monolayer at the air/water interface with 300 mM Na<sub>2</sub>SO<sub>4</sub> and the addition of 0 mM (orange), 25 mM (green) and 300 mM (blue) NaI to the subphase. The schematic diagram within the plot points to the two water populations around 3200 cm<sup>-1</sup> (more ordered water) and 3400 cm<sup>-1</sup> (less ordered water) b) The oscillator strengths at 3200 cm<sup>-1</sup> (orange) and 3400 cm<sup>-1</sup> (red) as a function of NaI in the presence of 300 mM Na<sub>2</sub>SO<sub>4</sub>. The error bars are calculated from standard deviations from three sets of measurements. Equation S3 was used to fit the data and Table S4 provides the fitting parameters. c) Schematic diagrams depicting the effects of SO<sub>4</sub><sup>2-</sup> and I<sup>-</sup> on the orientation of the two water populations at the air/PNiPAM/water interface at various I<sup>-</sup> concentrations. Water molecules around I<sup>-</sup> ions closest to the polymer/water interface become more aligned upon iodide adsorption to the surface, resulting in an increase in the 3400 cm<sup>-1</sup> oscillator strength. The water population probed by the 3200 cm<sup>-1</sup> peak is affected by iodide ions that become more hydrated in the presence of sulfate and essentially disrupt the alignment of water molecules in this layer. The black arrows indicate the water dipole orientation.

solutions, a monotonic increase in the oscillator strength of the  $3200\text{ cm}^{-1}$  peak is observed and is related to the change in the interfacial potential as iodide binds to the surface (see Figure S2c). By contrast, in pure  $\text{Na}_2\text{SO}_4$  solutions, the oscillator strength of the  $3200\text{ cm}^{-1}$  peak continuously decreases (see Figure S3). This decreasing trend is caused by the disruption in the alignment of water molecules further from the polymer surface as more well hydrated ions are introduced. Mixtures of  $\text{Na}_2\text{SO}_4$  with increasing concentrations of  $\text{NaI}$  first show a decrease in the  $3200\text{ cm}^{-1}$  peak before an increase is observed (see Figure 5b). That is, the addition of the weakly hydrated salt,  $\text{NaI}$ , initially has an impact on the VSFS intensity similar to that of  $\text{Na}_2\text{SO}_4$ . Iodide therefore behaves like a strongly hydrated ion and is responsible for the dip observed in the oscillator strength of the  $3200\text{ cm}^{-1}$  peak in the VSFS measurements of mixed salt solutions.

MD simulations of bulk salt solutions have been performed to quantify changes in iodide-water affinity ( $\Delta N$ ), defined here as

$$\Delta N = \frac{N_w}{V} \int_0^{r_2} [g_{\text{an},w}(r) - 1] 4\pi r^2 dr, \quad (2)$$

where  $g_{\text{an},w}(r)$  is the anion-water radial distribution function, and  $N_w/V$  is the number density of water molecules.  $\Delta N$  is determined by the balance of ion-water, ion-ion and water-water (hydrogen bonding) interactions and can be interpreted as the change in the number of water molecules in a spherical observation volume of radius  $r_2$  before and after placing an anion at the center of that region. In our analysis,  $r_2$  is the radius of the second hydration shell whose properties, as will be discussed below, are affected most in mixed salt solution. In this work we use the words more or less hydrated in the context of this definition. Specifically, more or less hydrated indicates a change in  $\Delta N$  in the presence of the background salt with respect to the absence of it. For comparison,  $\Delta N$  has been calculated not only for  $\text{I}^-$  but also for  $\text{Cl}^-$  in the presence and absence of  $\text{Na}_2\text{SO}_4$  background salt. Figure 6 (Figure S4, Figure S5 and Figure S6 for the first and second hydration shell separately)

shows that the anion-water affinities should be ranked  $\text{SO}_4^{2-} > \text{Cl}^- > \text{I}^-$ . Interestingly, the iodide-water affinity increases in the mixed salt system (see Figure 6a), while the chloride-water affinity (see Figure 6b) is not significantly affected by the presence of  $\text{Na}_2\text{SO}_4$  (see Supporting Information).

While the water affinity for iodide increases, its ion pairing affinity decreases in the presence of  $\text{Na}_2\text{SO}_4$  (Figure 7a, see Figure S7 for separate types of ion pairs). Analysis of ion pairing affinity, similar to Equation 2 and defined by Equation S5, provides a molecular mechanism for the increase in iodide hydration in the presence of  $\text{Na}_2\text{SO}_4$ . This analysis includes contact ion pairs (CIPs) and solvent shared ion pairs (SIPs).<sup>29</sup> As shown in Figure 7a and Figure 7c (see Figure S7 and Figure S8 for separate types of ion pairs), in the mixed salt case, some sodium ions from the introduction of NaI partition to the counterion cloud around sulfate. This leaves a lower excess density of counterions around iodide. Therefore, iodide ions become more hydrated in the presence of  $\text{Na}_2\text{SO}_4$ . This phenomenon is the origin of the flexible hydration shell around iodide. Such remarkable behavior for the weakly hydrated anion ( $\text{I}^-$ ) is schematically depicted in the TOC Figure as well as in Figure 1. Consequently, the background salt increases the NaI activity,<sup>29,30</sup> leading to the salting out effect observed in region I. Note, the anion-water and ion pairing affinities have been calculated from simulations conducted at 300 K. The same properties have also been calculated from simulations conducted at 285 K and 305 K. This also applies to other systems discussed later in this work. All three temperatures show the same trends for the anion-water ion pairing affinities (Figure S10) and imply that the molecular mechanism is robust. An increased pairing affinity between  $\text{SO}_4^{2-}$  and  $\text{Na}^+$  has also been experimentally observed in the presence of  $\text{NaClO}_4$ .<sup>31</sup> Since  $\text{ClO}_4^-$  is a weakly hydrated anion, it is expected to behave very similarly to  $\text{I}^-$ , implying that sodium ion affinity increases for sulfate when NaI is introduced into the solution, thus supporting the proposed mechanism in region I. The observed findings from the VSFS measurements and MD simulations for bulk solutions are depicted schematically in Figure 5c.

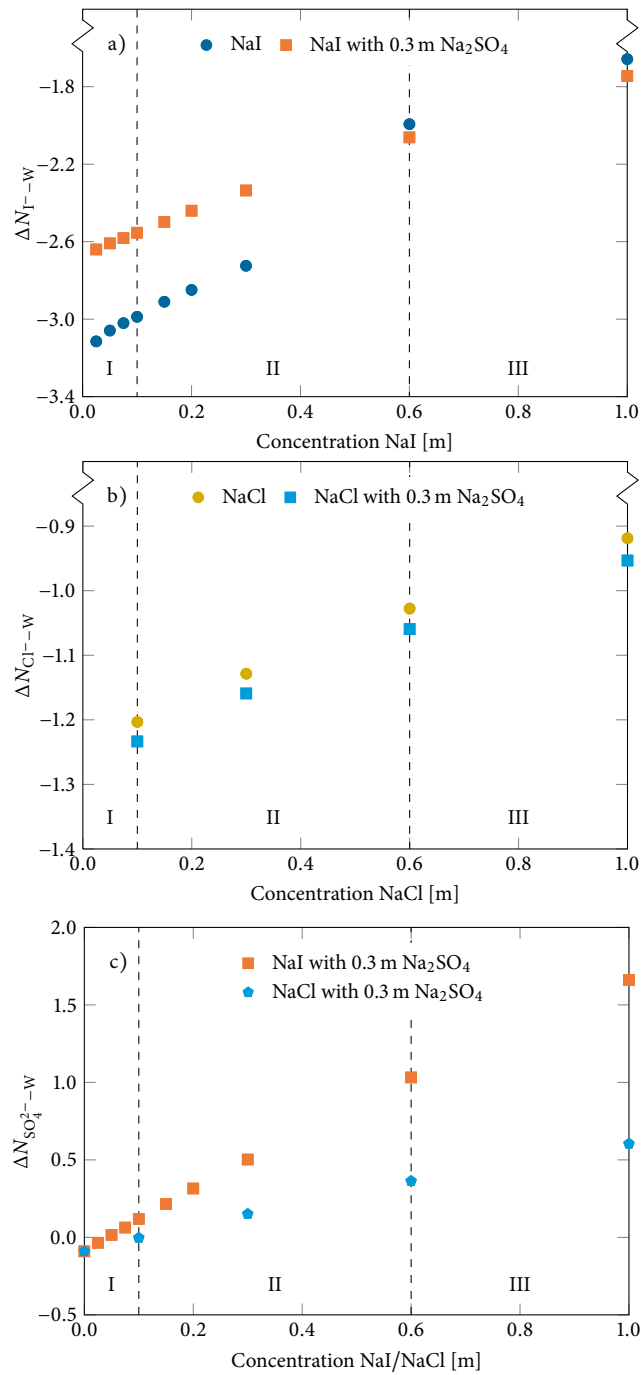


**Figure 6.** a) Iodide-water affinity as a function of NaI concentration in the absence (blue) and presence (orange) of  $\text{Na}_2\text{SO}_4$  as the background salt. b) Chloride-water affinity as a function of NaCl concentration in the absence (yellow) and presence (light blue) of  $\text{Na}_2\text{SO}_4$  as the background salt. c) Sulfate-water affinity as a function of NaI or NaCl concentration in mixtures of NaI with  $\text{Na}_2\text{SO}_4$  (orange) and NaCl with  $\text{Na}_2\text{SO}_4$  (light blue), respectively. The error bars are error estimates calculated from 20 blocks and sample standard deviations, and are smaller than the symbols.

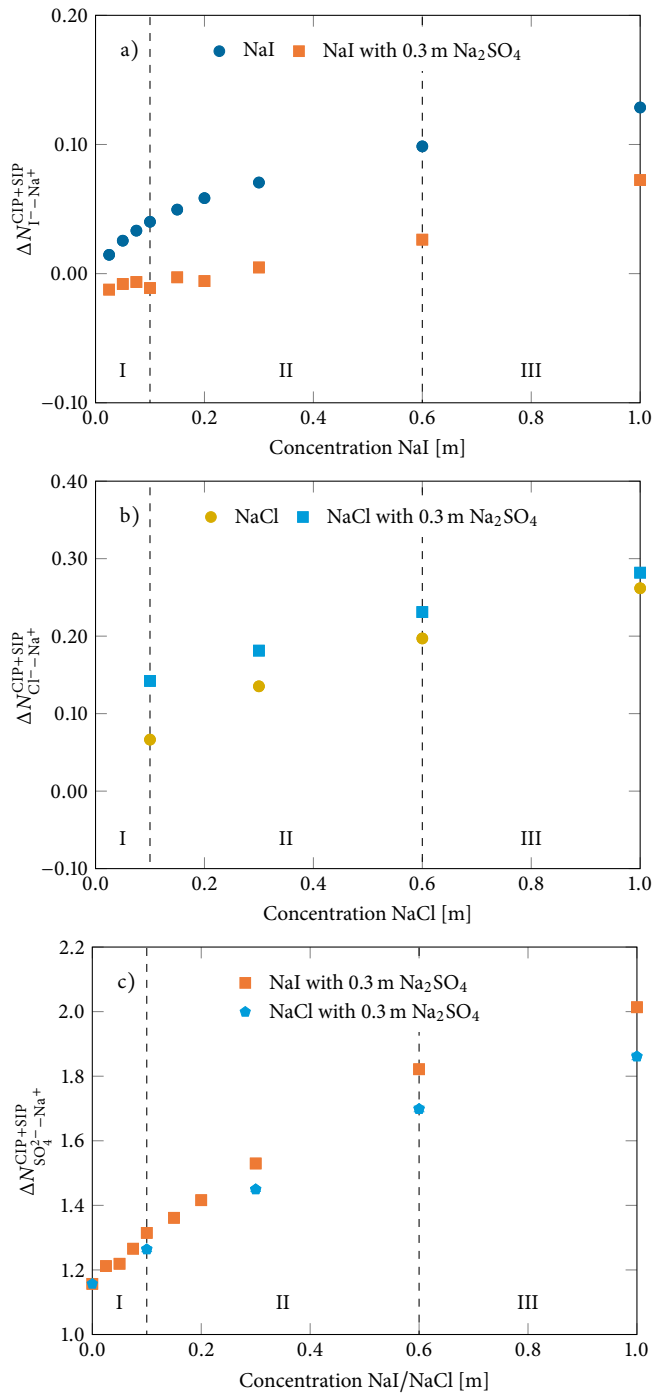


**Figure 7.** a) Excess ion pairing between iodide and sodium for both contact and solvent shared ion pairs (CIP+SIP) as a function of NaI concentration in the absence (blue) and presence (orange) of 0.3 m  $\text{Na}_2\text{SO}_4$ . b) Excess ion pairing between chloride and sodium for both contact and solvent shared ion pairs (CIP+SIP) as a function of NaCl concentration in the absence (yellow) and presence (light blue) of 0.3 m  $\text{Na}_2\text{SO}_4$ . c) Excess ion pairing between sulfate and sodium for both contact and solvent shared ion pairs (CIP+SIP) as a function of NaI or NaCl concentration in mixtures of NaI with  $\text{Na}_2\text{SO}_4$  (orange) and NaCl with  $\text{Na}_2\text{SO}_4$  (light blue), respectively. The error bars are error estimates calculated from 20 blocks and sample standard deviations, and are smaller than the symbols.

Additional LCST data measured in D<sub>2</sub>O (see Figure S11 and Table S5) also supports the conclusions drawn here. Indeed, because hydrogen bonds in D<sub>2</sub>O are stronger than in H<sub>2</sub>O, the balance of ion-water and water-water interactions shifts in favor of water-water interactions for heavy water. Hence, ion-water affinities are reduced in D<sub>2</sub>O, and Na<sub>2</sub>SO<sub>4</sub> has a smaller effect on the iodide-D<sub>2</sub>O affinity. Figure S11 explicitly shows that the LCST dip at low NaI concentrations is significantly reduced in D<sub>2</sub>O as compared to H<sub>2</sub>O.

**Ion specificity of polymer solubility in aqueous mixed salt solutions.** The ability of iodide to modulate its water affinity depends on the type and concentration of the background salt that is present in solution. With NaCl instead of Na<sub>2</sub>SO<sub>4</sub> as the background salt, adding NaI causes a substantially smaller dip in the LCST (Figure S12a and Table S6). This is expected, as the counter cation cloud around a divalent ion such as SO<sub>4</sub><sup>2-</sup> is substantially denser than the one around a monovalent ion like Cl<sup>-</sup>. In fact, the non-additive effect arises primarily from the valency of the background anion rather than its specific identity.<sup>32,33</sup> As such, the mixed salt effect with a divalent anion is substantially more pronounced than when both anions are monovalent (compare Figure 3b with Figure S12b). Moreover, the more effective partitioning of Na<sup>+</sup> from the counter cation cloud around I<sup>-</sup> to the one around SO<sub>4</sub><sup>2-</sup> (as opposed to the one around Cl<sup>-</sup>) concurs with the known pairing affinity between Na<sup>+</sup> and anions in single salt solutions following the series SO<sub>4</sub><sup>2-</sup> > Cl<sup>-</sup> > I<sup>-</sup> with dissociation constants of 150 mM,<sup>34</sup> 250 mM,<sup>35</sup> and 1.4 M,<sup>36</sup> respectively. With further increases in the NaI concentration, the LCST of PNiPAM shows a very subtle increase in region II followed by a decrease in region III (Figure S12). As the background anion, chloride is not as strongly hydrated as sulfate and cannot effectively salt out iodide. This results in a smaller driving force for iodide adsorption at the polymer/water interface. In fact, Figure S13 shows that fewer iodide ions are salted out to the surface of a PNiPAM 5-mer by NaCl than by Na<sub>2</sub>SO<sub>4</sub> (Figure 4), in agreement with a smaller  $B_{\max,1}$  value for chloride than for sulfate (Table S6 and Table 1). In region III, a salting out effect is observed due to the depletion of hydration ions from the polymer interface. This occurs because the polymer surface becomes saturated

with the weakly hydrated anion.

In order to demonstrate that the flexibility of the anion's hydration shell is essential for displaying non-additive behavior, we also ran experiments where NaI was switched for NaCl in the presence of  $\text{Na}_2\text{SO}_4$  as the background salt. Interestingly, there is no evidence for non-additivity in regions I and II (Figure S14 and Table S7). Figure 6 shows that chloride has higher water affinity than iodide with the same background salt. Moreover, the hydration shell around chloride is less flexible than the one around iodide (compare Figure 6a and Figure S4 with Figure 6b and Figure S5). Additionally, the water affinity for sulfate is less affected by NaCl than by NaI (Figure 6c and Figure S6). Analysis of the ion pairing affinity, defined by Equation S5, shows an increased pairing affinity between  $\text{SO}_4^{2-}$  and  $\text{Na}^+$  in the presence of NaCl. This has previously been observed experimentally.<sup>37</sup> However, the pairing affinity is less pronounced than in the presence of NaI (see Figure 7c and Figure S8 for separate types of ion pairs), originating from sodium pairing more strongly with chloride than with iodide. The partitioning of sodium to the counter cation cloud around sulfate does not occur (see Figure 7b and Figure 7c; see Figure S8 and Figure S9 for separate types of ion pairs) and thereby causes the hydration shell around chloride to be less flexible. This explains the shallower decrease in the LCST in region I of PNiPAM in mixtures of NaCl with  $\text{Na}_2\text{SO}_4$  (Figure S14) compared to systems with NaI (Figure 3). Essentially, both chloride and sulfate remain well hydrated and thus salt out the polymer by an excluded volume effect at all concentrations of NaCl (Figure S14).

**Non-additive ion effects are universal.** Other thermoresponsive polymers were investigated with mixed salts in addition to PNiPAM. A dip feature in the LCST could also be observed for poly(*N,N*-dimethylacrylamide) (PDMA) in mixtures of NaI with  $\text{Na}_2\text{SO}_4$  (Figure S15a) as well as for polyethylene glycol (PEG) in mixtures of NaSCN with  $\text{Na}_3\text{PO}_4$  (Figure S15b). See Table S8 for the fitting parameters. As such, the LCST behavior observed herein for PNiPAM with NaI and  $\text{Na}_2\text{SO}_4$  is expected to be quite generic. Interestingly, the magnitudes and positions of the dip clearly depends on polymer chemistry as well as on the

ion identities. Such differences are not unexpected since the driving forces for non-additivity of mixed salt solutions come from the competition between ion hydration in the bulk solution (universal behavior) and polymer-anion interactions, whereby the latter should be polymer specific.

## Conclusions

We have shown that the collapse and swelling of PNiPAM in aqueous solutions of mixed salts is determined by the subtle balance of ion hydration and direct interactions of weakly hydrated anions with the polymer. This balance can be significantly modulated by the presence of a strongly hydrated salt, which is depleted from the polymer/water interface. Mixing a fixed concentration of a strongly hydrated salt (i.e.  $\text{Na}_2\text{SO}_4$ ) with an increasing concentration of a weakly hydrated salt (i.e.  $\text{NaI}$ ) drives consecutive polymer collapse and polymer swelling transitions. On the one hand, polymer collapse is caused by a depletion effect arising from the weakly hydrated anion becoming more hydrated in the presence of the strongly hydrated salt. On the other hand, polymer swelling is the result of the weakly hydrated anion partitioning to the polymer/water interface. The origin of the bifurcated behavior of the weakly hydrated anion stems from the partitioning of the cation between the strongly and weakly hydrated anions. Moreover, the strongly hydrated anion salts out the more weakly hydrated anion, leading to an enhanced swelling effect at higher concentrations. The consecutive collapse and swelling transitions occur because the weakly hydrated anions have a flexible hydration shell, which can bind excess water in the bulk, but shed water molecules at the interface.

The work reported herein illustrates that non-additive ion effects in mixed salt solutions are caused by changes in the water affinity of anions which are traditionally considered to be weakly hydrated. The observed phenomenon requires these anions to relocate their position in the anion Hofmeister series toward the more strongly hydrated anions (see Figure 1).

This flexible hydration shell behavior, demonstrated for  $\text{I}^-$  in this work, is expected to also apply to  $\text{SCN}^-$  and  $\text{ClO}_4^-$  as well as other weakly hydrated anions. We expect that these new insights into Hofmeister ion chemistry will have consequences beyond the newly discovered effect on the aqueous polymer solubility reported herein. Moreover, it is likely that additional non-additive effects still remain to be discovered. This is quite significant, as the origins of the Hofmeister series in single salt solutions are just now beginning to be understood. Apparently, significantly more work will need to be done to understand the behavior of complex environments, like the solutions inside living cells, the brine solutions of ocean waters, as well as the numerous solutions employed in electrochemical setups, where dozens of different ions can be present simultaneously.

## Acknowledgement

The simulations for this research were conducted on the Lichtenberg high performance computer at the TU Darmstadt. Furthermore, the Darmstadt authors thank the LOEWE project from iNAPO which is funded by the Ministry for Higher Education, Research and the Arts (HMWK) of the state of Hessen. The Penn State authors thank the National Science Foundation (CHE-1709735) for support.

## Supporting Information Available

Methods, additional experimental data, additional simulation data, lower critical solution temperature fitting and vibrational sum frequency spectroscopy fitting.

## References

- (1) Hofmeister, F. Zur Lehre von der Wirkung der Salze. *Arch. für Exp. Pathol. und Pharmakologie* **1888**, *25*, 1–30.

(2) Kunz, W.; Henle, J.; Ninham, B. 'Zur Lehre von der Wirkung der Salze' (About the Science of the Effect of Salts): Franz Hofmeister's Historical Papers. *Curr. Opin. Colloid Interface Sci.* **2004**, *9*, 19–37.

(3) Jungwirth, P.; Tobias, D. J. Molecular Structure of Salt Solutions: A New View of the Interface with Implications for Heterogeneous Atmospheric Chemistry. *J. Phys. Chem. B* **2001**, *105*, 10468–10472.

(4) Zhang, Y.; Furyk, S.; Bergbreiter, D. E.; Cremer, P. S. Specific Ion Effects on the Water Solubility of Macromolecules: PNIPAM and the Hofmeister Series. *J. Am. Chem. Soc.* **2005**, *127*, 14505–14510.

(5) Cho, Y.; Zhang, Y.; Christensen, T.; Sagle, L. B.; Chilkoti, A.; Cremer, P. S. Effects of Hofmeister Anions on the Phase Transition Temperature of Elastin-Like Polypeptides. *J. Phys. Chem. B* **2008**, *112*, 13765–13771.

(6) Rembert, K. B.; Okur, H. I.; Hilty, C.; Cremer, P. S. An NH Moiety is Not Required for Anion Binding to Amides in Aqueous Solution. *Langmuir* **2015**, *31*, 3459–3464.

(7) Guggenheim, E. The Specific Thermodynamic Properties of Aqueous Solutions of Strong Electrolytes. *London, Edinburgh, Dublin Philos. Mag. J. Sci.* **1935**, *19*, 588–643.

(8) Guggenheim, E.; Turgeon, J. C. Specific Interaction of Ions. *Trans. Faraday Soc.* **1955**, *51*, 747–761.

(9) Brönsted, J. N. Studies on Solubility. IV. The Principle of the Specific Interactions of Ions. *J. Am. Chem. Soc.* **1922**, *44*, 877–898.

(10) Brönsted, J. N. The Individual Thermodynamic Properties of Ions. *J. Am. Chem. Soc.* **1923**, *45*, 2898–2910.

(11) Collins, K. D.; Washabaugh, M. W. The Hofmeister Effect and the Behaviour of Water at Interfaces. *Q. Rev. Biophys.* **1985**, *18*, 323–422.

(12) Pegram, L. M.; Record, M. T. Hofmeister Salt Effects on Surface Tension Arise from Partitioning of Anions and Cations Between Bulk Water and the air-water interface. *J. Phys. Chem. B* **2007**, *111*, 5411–5417.

(13) Pegram, L. M.; Record, M. T. Thermodynamic Origin of Hofmeister Ion Effects. *J. Phys. Chem. B* **2008**, *112*, 9428–9436.

(14) Schneider, C. P.; Shukla, D.; Trout, B. L. Arginine and the Hofmeister Series: The Role of Ion-Ion Interactions in Protein Aggregation Suppression. *J. Phys. Chem. B* **2011**, *115*, 7447–7458.

(15) Jungwirth, P.; Cremer, P. S. Beyond Hofmeister. *Nat. Chem.* **2014**, *6*, 261–263.

(16) Heyda, J.; Okur, H. I.; Hladíková, J.; Rembert, K. B.; Hunn, W.; Yang, T.; Dzubiella, J.; Jungwirth, P.; Cremer, P. S. Guanidinium can Both Cause and Prevent the Hydrophobic Collapse of Biomacromolecules. *J. Am. Chem. Soc.* **2017**, *139*, 863–870.

(17) Balos, V.; Bonn, M.; Hunger, J. Anionic and Cationic Hofmeister Effects are Non-Additive for Guanidinium Salts. *Phys. Chem. Chem. Phys.* **2017**, *19*, 9724–9728.

(18) Zajforoushan Moghaddam, S.; Thormann, E. Hofmeister Effect of Salt Mixtures on Thermo-Responsive Poly(propylene oxide). *Phys. Chem. Chem. Phys.* **2015**, *17*, 6359–6366.

(19) Ottosson, N.; Heyda, J.; Wernersson, E.; Pokapanich, W.; Svensson, S.; Winter, B.; Öhrwall, G.; Jungwirth, P.; Björneholm, O. The Influence of Concentration on the Molecular Surface Structure of Simple and Mixed Aqueous Electrolytes. *Phys. Chem. Chem. Phys.* **2010**, *12*, 10693–10700.

(20) van der Vegt, N. F. A.; Nayar, D. The Hydrophobic Effect and the Role of Cosolvents. *J. Phys. Chem. B* **2017**, *121*, 9986–9998.

(21) Morris, A. W.; Riley, J. P. The Bromide/Chlorinity and Sulphate/Chlorinity Ratio in Sea Water. *Deep Sea Res. Oceanogr. Abstr.* **1966**, *13*, 699–705.

(22) Nostro, P. L.; Ninham, B. W. Hofmeister Phenomena: An Update on Ion Specificity in Biology. *Chem. Rev.* **2012**, *112*, 2286–2322.

(23) Vo, B. S.; Shallcross, D. C. Modeling Solution Phase Behavior in Multicomponent Ion Exchange Equilibria Involving H+, Na+, K+, Mg2+, and Ca2+ Ions. *J. Chem. Eng. Data* **2005**, *50*, 1995–2002.

(24) Chen, X.; Yang, T.; Kataoka, S.; Cremer, P. S. Specific Ion Effects on Interfacial Water Structure near Macromolecules. *J. Am. Chem. Soc.* **2007**, *129*, 12272–12279.

(25) Du, Q.; Freysz, E.; Shen, Y. R. Vibrational Spectra of Water Molecules at Quartz/Water Interfaces. *Phys. Rev. Lett.* **1994**, *72*, 238–241.

(26) Richmond, G. L. Molecular Bonding and Interactions at Aqueous Surfaces as Probed by Vibrational Sum Frequency Spectroscopy. *Chem. Rev.* **2002**, *102*, 2693–2724.

(27) Kim, G.; Gurau, M.; Kim, J.; Cremer, P. S. Investigations of Lysozyme Adsorption at the Air/Water and Quartz/Water Interfaces by Vibrational Sum Frequency Spectroscopy. *Langmuir* **2002**, *18*, 2807–2811.

(28) Jena, K. C.; Hore, D. K. Variation of Ionic Strength Reveals the Interfacial Water Structure at a Charged Mineral Surface. *J. Phys. Chem. C* **2009**, *113*, 15364–15372.

(29) van der Vegt, N. F. A.; Haldrup, K.; Roke, S.; Zheng, J.; Lund, M.; Bakker, H. J. Water-Mediated Ion Pairing: Occurrence and Relevance. *Chem. Rev.* **2016**, *116*, 7626–7641.

(30) Hess, B.; van der Vegt, N. F. A. Cation Specific Binding with Protein Surface Charges. *Proc. Natl. Acad. Sci.* **2009**, *106*, 13296–13300.

(31) Luts, P.; Vanhees, J. L. C.; Yperman, J. H. E.; Mullens, J. M. A.; van Poucke, L. C. Potentiometric Investigation of NaSO<sub>4</sub><sup>-</sup> Ion Pair Formation in NaClO<sub>4</sub> Medium. *J. Solution Chem.* **1992**, *21*, 375–382.

(32) Knackstedt, M. A.; Ninham, B. W. Correlations and Thermodynamic Coefficients in Dilute Asymmetric Electrolyte Solutions. *J. Phys. Chem.* **1996**, *100*, 1330–1335.

(33) Guldbrand, L.; Jonsson, B. Electrical Double Layer Forces. A Monte Carlo Study. *J. Chem. Phys.* **1984**, *80*, 2221.

(34) Buchner, R.; Capewell, S. G.; Hefter, G.; May, P. M.; Di, V.; V, M. U. Ion-Pair and Solvent Relaxation Processes in Aqueous Na<sub>2</sub>SO<sub>4</sub> Solutions. *J. Phys. Chem. B* **1999**, *103*, 1185–1192.

(35) Eiberweiser, A.; Buchner, R. Ion-pair or Ion-Cloud Relaxation? On the Origin of Small-Amplitude Low-Frequency Relaxations of Weakly Associating Aqueous Electrolytes. *J. Mol. Liq.* **2012**, *176*, 52–59.

(36) Wachter, W.; Kunz, W.; Buchner, R. Is There an Anionic Hofmeister Effect on Water Dynamics? Dielectric Spectroscopy of Aqueous Solutions of NaBr, NaI, NaNO<sub>3</sub>, NaClO<sub>4</sub>, and NaSCN. *J. Phys. Chem. A* **2005**, *109*, 8675–8683.

(37) Manuela Santos, M.; Guedes de Carvalho, J. R. F.; Guedes do Carvalho, Carvalho, R. A. Determination of the Association Constant of NaSO<sub>4</sub><sup>-</sup> with the Sodium-Selective Electrode. *J. Solution Chem.* **1975**, *4*, 25–29.

# Graphical TOC Entry

